

Characteristics of possible neutral-heavy-lepton production in muon reactions

Carl H. Albright

*Fermi National Accelerator Laboratory, Batavia, Illinois 60510
and Department of Physics, Northern Illinois University DeKalb, Illinois 60115**

Robert E. Shrock

Physics Department, Princeton University, Princeton, New Jersey 08540

(Received 9 January 1979)

We study the production of a neutral heavy lepton by an incident muon via the reaction $\mu^\pm + N \rightarrow \bar{M}^0 + X$ followed by the decay $\bar{M}^0 \rightarrow \mu^- \mu^+ \dots$. We analyze the experimentally observable characteristics of the resulting dimuon pair and present distributions in final-muon energy, hadron energy, total visible energy, muon transverse momenta, and dimuon invariant-mass and azimuthal-angle correlations. On the basis of this study we formulate a set of cuts and tests which can be used to search for the dimuon signal from the \bar{M}^0 . The main features of various backgrounds are briefly discussed from the viewpoint of discriminating between them and the \bar{M}^0 signal. Our analysis is directly applicable to a current muon experiment being conducted by a Berkeley-Fermilab-Princeton collaboration.

I. INTRODUCTION

An old and still intriguing question in particle physics concerns the number and properties of leptons. At present the known leptons consist of the three pairs l^-, ν_l where $l^- = e^-, \mu^-$ and τ^- , with the existence of ν_τ being somewhat inferential. In the sequential Weinberg-Salam (WS) $SU(2) \times U(1)$ gauge theory of weak and electromagnetic interactions¹ these leptons are assigned to left-handed doublets and right-handed singlets; thus

$$\begin{pmatrix} \nu_l \\ l_l \end{pmatrix}_L, \quad (l_l)_R, \quad (1.1)$$

where $l = e, \mu, \tau$. This model is successful in accounting, with only one free parameter, for a wide variety of charged-current (CC) and neutral-current (NC) data,² including neutrino elastic and deep-inelastic semileptonic CC and NC reactions, low-energy and one high-energy leptonic NC experiments,³ and, quite impressively, with the recent high-precision polarized-electron scattering experiment at SLAC.⁴ The situation with the search for parity violation in heavy atoms is indecisive,⁵ first because of disagreements among the experiments, and secondly because of the difficulty of calculating reliably the effect expected from a given model for an atom as heavy as ¹²⁶Bi. Thus, it may well be that the sequential WS model, with some number, n , of quark doublets and an equal number of lepton doublets, will provide a correct description of weak interactions at energies attainable in the near future. The version of the model with three quark and lepton doublets, first discussed by Kobayashi and Maskawa,⁶ successfully incorporates the τ lepton⁷ and T-constituent quark, b .⁸ It also may be that

there are not very many additional fermions to be discovered; it has been estimated⁹ from astrophysical considerations of primordial helium production that the number of massless neutrinos is bounded by $n \leq 4$. If indeed the sequential WS model is correct, then two obvious but far-reaching consequences are that (a) the only neutral leptons are massless neutrinos and (b) the only charged-current coupling of a lepton l_i is to its own neutrino, ν_i .

However, since inferences about the higher-mass portion of the lepton spectrum based on the known leptons and their weak couplings are necessarily indirect, it still seems useful to investigate all direct experimental methods which might possibly be feasible in searching for and studying these heavy leptons. For example, it may yet be necessary to consider gauge groups larger than $SU(2) \times U(1)$; in this case there would presumably be charged and neutral heavy leptons which would couple weakly to each other and perhaps also to light leptons. In this paper we shall analyze one particular method, using muon reactions, of probing for the existence, and determining the properties, of possible neutral heavy leptons. Of course we are acutely aware of the inferential evidence, from the current success of the WS model, against the existence of nonsequential heavy leptons; accordingly this study is intended to be exploratory rather than exhaustive.

One important motivation for undertaking this work at the present time is that data will soon be forthcoming from a Berkeley-Fermilab-Princeton (BFP) muon scattering experiment at Fermilab.¹⁰ Among the original purposes of this experiment was the search for neutral heavy leptons produced weakly by muons. Correspondingly, a crucial feature of the BFP apparatus is

a fine-grained hadron calorimeter. As is well known, hadron calorimetry is generally an unnecessary luxury in an experiment to study deep-inelastic inclusive electron or muon scattering, since measurements of the energy and angle of the scattered lepton suffice to reconstruct the kinematics completely. However, to search for heavy-lepton production such hadron calorimetry is essential, because it enables one to test for substantial missing energy [due to outgoing neutrino(s)], a key signature of the decay of a heavy lepton. Such hadron calorimetry was not utilized in the previous muon scattering experiments at Fermilab, by the Michigan State-Cornell,¹¹ Michigan State,¹² and Chicago-Harvard-Illinois-Oxford¹³ collaborations. Further data which may yield information on the question of heavy-lepton production will be obtained by two muon experiments underway at CERN SPS.^{14,15}

As a technique for investigating weak interactions and, in particular heavy-lepton production, muon reactions have one overwhelming problem: in contrast to neutrinos, which scatter only weakly, practically all muons scatter electromagnetically rather than weakly. Specifically, heavy-lepton production occurs at a relative rate which is given approximately by

$$\frac{(\partial^2\sigma/\partial Q^2\partial\nu)(\mu+N\rightarrow M+X)}{(\partial^2\sigma/\partial Q^2\partial\nu)(\mu+N\rightarrow\mu+X)} \sim \frac{G_F^2 Q^4 \rho}{8\pi^2 \alpha^2}, \quad (1.2)$$

where Q^2 and ν are the four-momentum transfer squared and the energy transfer, respectively, and ρ represents a phase-space suppression factor for heavy-lepton and possible accompanying heavy-quark production. For $Q^2 = 25 \text{ GeV}^2$ and $\rho = 0.5$, the ratio (1.2) $\sim 1 \times 10^{-5}$. The actual multimMuon signal observed in the experiment will be further reduced by a branching ratio of ~ 0.1 to $\sim 1 \times 10^{-6}$. Evidently, extreme care is therefore necessary in order to discriminate between multimMuons arising from heavy-lepton and possible heavy-quark decay, and those arising from the many backgrounds. As will be clear from our study, there are several powerful cuts and tests which can be applied for this purpose. For the case of neutral-heavy-lepton production, upon which we shall concentrate, these include (1) final-state muon topology: $\mu^- \mu^+$; (2) $E_{\mu^\pm} > 20 \text{ GeV}$; (3) hadronic energy deposition $E_H > 20 \text{ GeV}$; (4) $Q_{\text{vis}}^2 > 10-15 \text{ GeV}^2$; (5) the Pais-Treiman test¹⁶: $0.48 < \langle E_{\mu^-} \rangle / \langle E_{\mu^+} \rangle < 2.1$; (6) the invariant mass of the dimuon pair, $M_{\mu\mu} \geq 1 \text{ GeV}$ and less than an upper bound which is energy-independent; and (7) the transverse momentum of the opposite-sign muon is greater than $\sim 1 \text{ GeV}$. There are also other tests which involve the subtraction of the number of same-sign di-

muon events from the raw number of opposite-sign events, the azimuthal angles between the μ^- and μ^+ , and the analysis of twofold correlations among the transverse momenta, invariant mass, and azimuthal angles characterizing the dimuons.

It should be emphasized that a number of these tests would not be possible with a neutrino beam. Perhaps most notably, the test for missing energy and corresponding cut rely upon the fact that the energy of the incident muons is known quite accurately, to $\sim 0.5\%$, in sharp contrast with the situation in neutrino experiments. Secondly, since the flux spectrum for a typical neutrino beam peaks at 20-25 GeV and falls sharply for higher energy, the majority of incident neutrinos cannot produce a heavy lepton of mass greater than a few GeV. However, a typical muon beam energy is 225 GeV, and hence there is much less kinematic suppression of heavy-lepton production. Thirdly, there is the possibility of varying the incident muon energy and measuring the resultant changes in various kinematic distributions in order to test whether the dimuons originate from a common lepton parent or not. Another property of muon reactions which may be helpful in isolating weak effects is the possibility of reversing the muon polarization without charge-conjugating the muon. Thus muon reactions have a number of features for the study of heavy-lepton production which may motivate one to impose the extremely demanding cuts necessary to offset their one great disadvantage, namely the tiny relative rate.

There are six general types of elementary muon-induced weak heavy lepton production reactions:

$$\mu^- + q \rightarrow M^0 + q', \quad (1.3a)$$

$$\mu^- + q \rightarrow M^0 + Q, \quad (1.3b)$$

$$\mu^- + q \rightarrow M^{--} + q', \quad (1.4a)$$

$$\mu^- + q \rightarrow M^{--} + Q, \quad (1.4b)$$

$$\mu^- + q \rightarrow M^- + q', \quad (1.5a)$$

$$\mu^- + q \rightarrow M^- + Q, \quad (1.5b)$$

together with the corresponding reactions with incident μ^+ , where q denotes the initial struck quark and q' and Q denote final light and heavy quarks, respectively. As is clear from Eqs. (1.3)-(1.5) we consider only deep-inelastic inclusive muon reactions, since these are the only ones of experimental interest. At this point we shall use some theoretical guidance in choosing a process upon which to concentrate. Reactions (1.4a), (1.4b) involve doubly charged heavy leptons, which do not appear in practically any

viable weak-interaction models. Reactions (1.5a), (1.5b) require tree-level nondiagonal neutral currents, which can often lead to conflict with such constraints as the $K_L K_S$ mass difference in the quark sector, and the upper bounds on muon-number violating processes such as $\mu \rightarrow e\gamma$ and $\mu \rightarrow ee\bar{e}$ in the lepton sector. This is not to say that nondiagonal neutral currents will necessarily lead to such disasters,¹⁷ but certainly a theory is much safer without them. Therefore, of the three possible types of muon-induced reactions, processes (1.3a) and (1.3b) seem to be the most likely to occur, if any of them do. Accordingly, we shall restrict our study to these reactions.

This paper is organized as follows. In Sec. II we discuss the present status of searches for neutral heavy leptons. Section III contains the details of our calculations, while Sec. IV presents our results. A brief analysis of the main backgrounds, and our concluding comments, are given in Sec. V.

II. STATUS OF SEARCHES FOR NEUTRAL HEAVY LEPTONS

Since we are interested here in muon reactions as a tool for producing and studying M^0 's, it is appropriate to ask first what is already known experimentally about such heavy leptons and whether there are other, more promising, ways of searching for them.

Regarding direct experimental searches for L^0 's (where $L^0 = E^0$ or M^0), consider as a first method production via e^+e^- annihilation. Depending on the beam energy and the masses and couplings involved, either the reaction $e^+e^- \rightarrow L^0\nu_e, \bar{L}^0\nu_e$ or $e^+e^- \rightarrow L^0\bar{L}^0$ would give the leading contribution to direct L^0 production. Since both processes have cross sections of order $G_F^2 s$, where s is the center-of-mass energy squared, they would occur with very small rates, at least for the values of s attainable at PETRA and PEP. There is, however, another, probably better, way of searching for L^0 's, namely as decay products of L^- 's or hadrons composed of heavy quarks, produced via the usual reaction $e^+e^- \rightarrow L^+L^-$ or $Q\bar{Q}$. In many models the L^0 would have among its various decay modes the channel $L^0 \rightarrow (\mu^- \text{ or } e^-)\pi^+$, which would yield a peak in the $(\mu^- \text{ or } e^-)\pi^+$ invariant-mass distribution. Such an experiment has been carried out at SPEAR.¹⁸ The (\bar{L}^0) 's were sought via the production and decay chain $e^+e^- \rightarrow \tau^+\tau^-; \tau^+ \rightarrow (\bar{L}^0)_+ \dots; (\bar{L}^0)_+ \rightarrow (\mu \text{ or } e)^+\pi^+$. A null result was obtained, which implies that there is no L^0 with mass less than ~ 1.5 GeV and the required couplings. This method

can also be used at the next generation of e^+e^- colliding beam machines to look for L^0 's as the decay products of b -flavored and perhaps heavier hadrons, and charged leptons which are higher in mass than τ .

From neutrino experiments there is considerable evidence against an M^0 which couples to ν_μ with more than a small fraction of full weak strength. The actual experimental upper bound applies to the maximum fraction of observed dilepton events which might consistently arise from M^0 production rather than charm production. This upper bound is of order 5–10% of the total dilepton signal, and yields a correlated upper bound on the $\nu_\mu M^0$ coupling strength as a function of the M^0 mass.¹⁹ The characteristics which were used to distinguish dilepton events due to charm production from those due to M^0 production have been discussed in detail in the literature.²⁰ However, it must be recalled that from a purely empirical point of view, the absence of a sizeable $\nu_\mu M^0$ coupling implies nothing about the existence or properties of a possible $\mu^+ M^0$ vertex, which is the crucial coupling for M^0 production in muon reactions.

Finally, there has been a beam-dump experiment²¹ which searched for long-lived L^0 's from 400-GeV proton-nucleus collisions. The experiment was sensitive to L^0 's which are produced unaccompanied by muons of momentum greater than 10 GeV and which decay via the mode $L^0 \rightarrow (\mu^- \text{ or } e^-)\pi^+$, with lifetimes in the range $10^{-10} < (\tau/\text{sec}) < 10^{-8}$. Since the type of M^0 which is relevant for muon experiments would normally be produced in conjunction with a muon, and since an L^0 of mass 2 GeV or larger would typically have a lifetime smaller than $\sim 10^{-13}$ sec, this experiment was not sensitive to the kind of M^0 of interest in the present study. A null signal was observed in the experiment, yielding an upper limit on the production cross section of an L^0 which satisfies the criteria listed above, and in addition has $m(L^0) < 1$ GeV, $x_F < 0.2$, and $\theta_{\text{lab}} < 10$ mrad, of $\sigma B < 2.8 \times 10^{-35}$ cm²/nucleon, at the 90% confidence level, where B denotes the branching ratio for $L^0 \rightarrow (\mu^- \text{ or } e^-)\pi^+$.

From this brief survey of past searches for neutral heavy leptons and of possible new methods of looking for them, it is clear that, in principle, muon reactions do have the capability of yielding useful information on the existence of M^0 's which couple to muons. We next proceed to the calculations.

III. CALCULATIONS

The differential cross section for the reaction $\mu^+ N \rightarrow (\bar{M}^0) X$ is

$$\frac{\partial^2 \sigma}{\partial x \partial y} = \frac{G_F^2 m_N E}{\pi} \left\{ \left(xy + \frac{m^2}{2m_N E} \right) y F_1 + \left(1 - y - \frac{m_N xy}{2E} - \frac{m^2}{4E^2} \right) F_2 - \eta y \left(x(1 - \frac{1}{2}y) - \frac{m^2}{4m_N E} \right) F_3 \right. \\ \left. + \frac{m^2}{m_N^2} \left[\left(\frac{m_N xy}{2E} + \frac{m^2}{4E^2} \right) F_4 - \left(\frac{m_N}{2E} \right) F_5 \right] \right\}, \quad (3.1)$$

where m_N (m) is the nucleon (M^0) mass, E (E') denotes the laboratory energy of the μ^+ (\bar{M}^0), $q^2 = -Q^2$ and $\nu = E - E'$ are the momentum transfer squared and laboratory energy transfer, and $x = Q^2/(2m_N \nu)$ and $y = \nu/E$ are the usual scaling variables. The constant η takes on the values $\eta = \pm 1$ for like and opposite quark and lepton helicities, respectively. There will, of course, be nonscaling effects due to the heavy-lepton production. In addition, if a heavy quark of mass m_Q is produced, there is further nonscaling behavior; in this case the structure functions are approximately functions of the variable²²

$$\xi = x + \frac{m_Q^2}{2m_N \nu}, \quad (3.2)$$

rather than just of x . Using ξ to subsume both the cases of light- and heavy-quark production, one can write the usual parton-model relations satisfied by the structure functions as²³

$$F_2(\xi) = 2\xi F_1(\xi), \quad (3.3)$$

$$-\xi F_3(\xi) = F_2(\xi), \quad (3.4)$$

$$\xi F_5(\xi) = F_2(\xi), \quad (3.5)$$

and

$$F_4(\xi) = 0. \quad (3.6)$$

There are corrections to these relations arising from the strong interactions and transverse momenta of the quarks, but for our purposes the standard relations are quite adequate.

The structure functions are expressed in terms of parton distributions, for which we use the following modified Pakvasa-Parashar-Tuan parametrization²⁴:

$$u(x) = u_v(x) + f_{\text{sea}}(x), \quad (3.7)$$

$$d(x) = d_v(x) + f_{\text{sea}}(x), \quad (3.8)$$

$$x[u_v(x) + d_v(x)] = 1.79 \sqrt{x} (1-x)^3 (1+2.3x) \\ + 1.11 \sqrt{x} (1-x)^{3.1}, \quad (3.9)$$

$$x\bar{u}(x) = x\bar{d}(x) = x\bar{s}(x) = x\bar{c}(x) = x f_{\text{sea}}(x) \\ = 0.13(1-x)^7, \quad (3.10)$$

where the subscript "v" denotes "valence." Our conclusions do not depend significantly on the particular details of this parametrization and would remain essentially the same if we had used another set of parton distributions which fits the

eN and $(\nu, \bar{\nu})N$ data well, such as that due to Field and Feynman.²⁵

The differential cross section given in Eq. (3.1) applies if the (\bar{M}^0) spin is summed over, and will be used for our calculation of the total M^0 production cross section. However, we shall naturally concentrate upon the experimentally observable final lepton state, and shall assume that the M^0 has among its decay modes the dimuon channel

$$M^0 \rightarrow \mu_{\chi_1}^- \mu_{\chi_2}^+ (\nu_\mu)_{\chi_2}, \quad (3.11)$$

where χ_i , $i = 1, 2$ denote the chiralities of the two lepton-vector-boson vertices involved in the decay. The branching ratio for this mode is, of course, model-dependent; typically, for $m_{M^0} = 4$ GeV, it would be $\sim 10\%$, and commensurately less for larger values of m_{M^0} . It is our intent to concentrate here on general model-independent kinematic signatures of M^0 production and decay to dimuons rather than more model-dependent features. In particular, we will not consider decay modes of the M^0 involving four charged leptons, since these would presumably have quite small branching ratios. Further, in the cases where a heavy quark is produced, its semileptonic decay will yield an additional muon roughly 10–20% of the time. Since this is a small correction to the already rare basic process $\mu^+ N - (\bar{M}^0) X$; $(\bar{M}^0)^0 - \mu^- \mu^+ \dots$, we shall neglect such additional muons. This is not to imply that these muons could not be distinguished from those arising from the M^0 decay; indeed several tests which could be used for these purposes have been discussed previously.^{26,27}

In order to calculate the kinematic distributions characterizing the dimuon spectra we carry out a Monte Carlo calculation, folding together the differential production cross section for a polarized (\bar{M}^0) with its differential decay distribution. For the production we shall consider three cases which serve to illustrate various different kinematical features. The most interesting reaction, if it occurs, is case (A), which, in terms of elementary fermions, is

$$(A): \mu_R^+ + d_L - \bar{M}_R^0 + u_L. \quad (3.12)$$

Our labelling of fermion chiralities is such as to indicate the type of vertex by which the particles can interact. Thus μ_L^- and μ_R^+ have helicity $\eta_i = -1$

while μ_R^- and μ_L^+ have $\eta_l = +1$. In this and all other cases we shall assume an isoscalar target, since this is the type of target used in the BFP experiment. Thus reaction (A) in terms of physical particles reads

$$\mu_R^+ + N \rightarrow \bar{M}_R^0 + X, \quad (3.13)$$

where N denotes an isoscalar nucleon. This reaction requires a $\mu_R^+ M_R^0$ coupling mediated by the usual W boson; we are, of course, aware that there is evidence against such a coupling, at full strength, from the SLAC polarized electron scattering experiment.⁴ However, from the point of view of rate, reaction (A) is the most promising way to produce $(\bar{M})^0$'s with muon beams. Corresponding to reaction (A) there is also the process with incident μ_R^- , which we label as case

$$(A'): \mu_R^- + u_L \rightarrow M_R^0 + d_L. \quad (3.14)$$

For $s = m_N^2 + 2m_N E \gg m_{M^0}^2$ the ratio of cross sections for reactions (A) and (A') is

$$\left. \frac{\sigma_{(A')}}{\sigma_{(A)}} \right|_{s \gg m_{M^0}^2} \simeq \frac{\sigma_{\nu N}}{\sigma_{\nu N}} \simeq 0.48 \quad (3.15)$$

(independent of energy, as long as the above condition is satisfied). This is a consequence of the fact that the leptons and valence quarks have the same helicities in case (A), but opposite helicities in case (A'), together with the appropriate correction due to sea quarks; in the absence of the latter the ratio would be $\frac{1}{3}$. Reaction (A) takes advantage of the leading particle effect in the primary proton-nucleon collision, which implies that there are more π^+ 's and K^+ 's produced than their antiparticles, and hence also more μ^+ 's than μ^- 's. For the operating conditions of the BFP experiment the relevant ratio is²⁸

$$\left. \frac{N(\mu^-)}{N(\mu^+)} \right|_{E=225 \text{ GeV}} \simeq 0.25. \quad (3.16)$$

Hence the actual event rate for case (A) is roughly eight times greater than that for case (A'). Despite this suppression, case (A') provides a useful contrast to case (A) because of the different helicities of the leptons and quarks; we shall not include it in our graphical presentation of results but will have further comparative comments to make on it at appropriate points. Both reactions (A) and (A') involve light-quark-to-light-quark transitions and therefore can be classified conveniently as (L, q) processes.²⁷ They thus have the merit of avoiding the kinematic suppression attendant upon heavy-quark production. Although this is of less crucial importance for muon, as opposed to neutrino, reactions because of the much higher incident energy, it is

certainly a useful feature.

The helicity of the μ^\pm is a very important factor in determining the type of $(\bar{M})^0$ production reaction. Since the μ^\pm is produced by the decay $\pi^\pm \rightarrow \mu^\pm (\bar{\nu})_\mu$ and, to a somewhat lesser extent, by the decay $K^\pm \rightarrow \mu^\pm (\bar{\nu})_\mu$, both of which involve purely left-handed weak vertices, in the rest frame of the decaying pseudoscalar meson this μ^\pm will be polarized oppositely to its preferred helicity, i.e., the μ^- (μ^+) will have helicity $+1$ (-1). If the Lorentz boost from this frame to the lab is in the direction of the velocity of the μ , as it is for the high-energy portion of the muon spectrum, then this helicity is retained. These high-energy muons will only interact via a right-handed vertex when they reach the target. Thus the highest-energy muon reactions are sensitive only to the right-handed couplings of the muon. This fact underlies the choice of muon chirality in cases (A) and (A').

It may be, however, that the lepton and quark couplings are such that there are no (L, q) $(\bar{M})^0$ production reactions. In this case the only available means of producing $(\bar{M})^0$'s with the highest-energy muons would be via one or both of the following generic types of (L, Q) processes:

$$\mu_R^+ + d_R \rightarrow \bar{M}_R^0 + Q(\frac{2}{3})_R \quad (3.17)$$

or

$$(B) \mu_R^- + u_R \rightarrow M_R^0 + Q(-\frac{1}{3})_R, \quad (3.18)$$

where $Q(q)$ represents some heavy quark of charge q which is assumed to couple to u_R or d_R by a (new) charged current. We shall assume for definiteness that this heavy quark is either the T constituent, b , with mass $m_b \simeq 4.7$ GeV and charge $-\frac{1}{3}$ or a charge $\frac{2}{3}$ quark, which will be denoted as t . Since there is good evidence that, given the assumed existence of the t quark, $m_t > m_b$, reaction (3.17) will suffer more kinematic suppression, relative to the background electromagnetic process $\mu^+ + N \rightarrow \mu^+ + X$ than will reaction (3.18) relative to its corresponding background process $\mu^- + N \rightarrow \mu^- + X$. We therefore choose the latter reaction, (3.18), as our illustrative example of a muon-induced (L, Q) M^0 production process and denote it henceforth as case (B). As was true of reaction (A') vis à vis reaction (A), reaction (B) has a cross section which is suppressed by roughly a factor of 4 by the leading-particle effect. However, the most important quantity is not the event rate, assuming that there are a nonzero number of M^0 events, but rather the ratio of the signal to the electromagnetic background, and in this ratio the different numbers of μ^+ as compared to μ^- cancel out. Since a wealth of neutral-current data indicates that, within the

context of $SU(2) \times U(1)$ models, u_R and d_R are singlets, it is quite likely that reaction (B) must be mediated by a new gauge boson, and thus requires an enlarged gauge group of weak and electromagnetic interactions. Accordingly, the effective strength of the current-current coupling is not definitely known. We shall assume that it is equal to that for a similar reaction mediated by the regular W ; our results can easily be scaled to be applicable to a particular model. Note that we again choose the helicity of the muon to be that of the high-energy component of the muon flux; this is simply to take full advantage of the available energy to counteract the kinematic suppression in an (L, Q) reaction.

Finally, there is the possibility that the muon has no right-handed couplings to M^0 . In this case M^0 production would have to rely entirely upon an assumed new left-handed coupling of the form $\mu_L^- M_L^0$, and hence upon the low-energy component of the muon flux, which has had its helicity reversed back to the "preferred" value of -1 ($+1$) for μ^- (μ^+) by the Lorentz transformation from the rest frame of the parent pseudoscalar meson (in which frame it was emitted opposite to the beam direction) to the lab frame. Although it is possible to construct $SU(2) \times U(1)$ models which feature such a $\mu_L^- M_L^0$ coupling, these models are quite artificial, since one must choose certain mixing angles carefully in order to avoid conflict with μ - e and hadron-lepton universality. Thus a $\mu_L^- M_L^0$ vertex tends to require an enlarged gauge group and would be mediated by a new gauge boson. In order to avoid contradiction with low-energy phenomenology such a new gauge boson must, aside from small mixing effects, couple light fermions to heavy ones. Accordingly, the $\mu_L^- + N \rightarrow M_L^0 + X$ reaction probably must involve heavy-quark production. However, if the high-energy component of the muon beam, defined as the muons which were emitted at 0° relative to the beam direction, has an energy of 225 GeV, as it does in the BPF experiment, then the low-energy, "preferred" helicity component, assumed to have been emitted at 180° relative to the beam direction in the parent meson rest frame, has a lab energy of ~ 129 GeV. At such a low energy the (L, Q) reaction would suffer very substantial kinematic suppression. Indeed, if there were even small mixing which led to a light-quark-to-light-quark transition, the resulting reaction could dominate over the (L, Q) one. We shall assume that this is the case and thus choose the reaction

$$(C): \mu_L^- + u_L \rightarrow M_L^0 + d_L \quad (3.19)$$

as our illustrative example of M^0 production by

the low-energy, "preferred" helicity component of the muon beam. This reaction will be denoted (C), as indicated.

It is necessary next to specify how the M^0 decays to a dimuon final state in the three cases under consideration. The chiralities which characterize the two vertices in the M^0 decay are correlated with the type of production reaction. For cases (A) and (A') the decay is mediated by the usual W boson and has the form

$$(A), (A'): (\overline{M}^0)_R \rightarrow \mu_R^\pm \mu_L^\mp (\overline{\nu})_{\mu L}. \quad (3.20)$$

For cases (B) and (C) the M^0 decay proceeds via a new virtual gauge boson; in keeping with the phenomenological orientation of the present study, we shall not make any detailed examination of various enlarged gauge groups, but instead shall simply assume that the decays have the forms

$$(B): M_R^0 \rightarrow \mu_R^- \mu_L^+ \nu_{\mu L} \quad (3.21)$$

and

$$(C): M_L^0 \rightarrow \mu_L^- \mu_L^+ \nu_{\mu L} \quad (3.22)$$

for these two cases.

These then, are the three types of (\overline{M}^0) production and decay which we shall consider. The final ingredient in the calculation is the M^0 mass; in order to illustrate the effect of varying this parameter, we take the two values $m_{M^0} = 4$ GeV and $m_{M^0} = 8$ GeV for our analysis. We proceed to describe our results.

IV. RESULTS

In this section we shall present various experimentally observable spectral distributions for the $\mu^+ \mu^-$ resulting from the (\overline{M}^0) production and decay process $\mu^\pm N \rightarrow (\overline{M}^0) X$; $(\overline{M}^0) \rightarrow \mu^- \mu^+ \dots$. The behavior of the total cross section for ν_μ - and $\overline{\nu}_\mu$ -induced heavy-lepton production with and without concomitant heavy-quark production has been discussed previously.²⁹ Many of the old results (excluding, of course, flux-averaged quantities) can be taken over and applied to μ^\pm -induced (\overline{M}^0) production. It has been shown that the cross section rises rapidly as the incident lepton energy E increases beyond the threshold value E_{th} , and curves over to approach a linear rise with energy. As was mentioned before, an important corollary of this behavior is that muon reactions have the great advantage, as compared with neutrino reactions, that the beam energy is much higher, typically 225 GeV instead of an average neutrino energy of 25–30 GeV. Hence there is much less kinematic suppression in producing a heavy lepton, especially one accompanied by a heavy quark, if one uses a muon beam rather than a

neutrino beam. Because of the strong threshold behavior of the cross section for (L, q) and, even more strikingly, (L, Q) reactions, it is certainly easier, from the point of view of rate alone, to produce an $(\bar{M})^0$ the smaller its mass is. However, the characteristic signatures which one will use to try to distinguish a dimuon signal arising from an $(\bar{M})^0$ apart from one arising from various background sources are much more distinctive for an $(\bar{M})^0$ with greater mass. Hence the combined chances for production and detection are probably comparable for $(\bar{M})^0$'s with larger or smaller masses, assuming, of course, that E is a reasonable distance above E_{th} .

We consider now the Q_{vis}^2 and ν , or equivalently, x_{vis} and y distributions. In neutrino-induced heavy-lepton production, since one does not know E and does not directly observe the heavy lepton, it is not possible to determine Q^2 , x , or y . In contrast, in muon-induced heavy-lepton production processes, although one still does not observe the heavy lepton directly, and hence cannot reconstruct Q^2 from E_{M^0} and θ_{M^0} , one can measure E_H (as in the neutrino case) and, knowing E precisely, can therefore determine y . The y distribution for muon-induced heavy-lepton production processes is thus an experimentally measurable quantity, as it was not for the analogous neutrino processes. On general kinematic grounds, for an (L, q) reaction the ν distribution is peaked toward small values in order to maximize the energy transfer to the heavy lepton.²⁹ As was shown in Ref. 27, for (L, Q) reactions there is a competition between maximizing the energy transfer to the heavy lepton L and to the heavy quark Q . The relative masses of L and Q , and to some extent, also the chiral structure of the quark and lepton vertices, determine which of these competing tendencies is dominant. The Q^2 distribution for (L, q) and (L, Q) reactions shows some peaking toward smaller values of Q^2 , but not so much as to prevent one from making the cut $Q_{vis}^2 > Q_0^2$, where $Q_0^2 \approx 10-15 \text{ GeV}^2$. This cut is very effective in eliminating the great majority of events from the electromagnetic reaction $\mu^\pm N \rightarrow \mu^\pm X$, together with the associated background sources of dimuons, since the differential cross section for the electromagnetic reaction falls off quite sharply, like Q^{-4} , as a function of Q^2 (which is equal to Q_{vis}^2 here).

In order to provide perspective for the numerical results it is useful to consider an approximate analytical treatment of the y distribution for $(\bar{M})^0$ production, with E sufficiently high that $(m_{M^0}^2/s) \ll 1$ for (L, q) reactions or $(m_{M^0} + m_Q)^2/s \ll 1$ for (L, Q) reactions. In this case, neglecting small ($\sim 10\%$) asymptotic freedom scaling devia-

tions, the y distribution can be written as

$$\frac{1}{\sigma} \frac{d\sigma}{dy} = \begin{cases} \frac{Q + \bar{Q}(1-y)^2}{Q + \bar{Q}/3}, & \text{for } \eta = 1 \\ \frac{Q(1-y)^2 + \bar{Q}}{Q/3 + \bar{Q}}, & \text{for } \eta = -1 \end{cases} \quad (4.1a)$$

$$\quad (4.1b)$$

where, in accordance with standard notation, Q and \bar{Q} denote the integrated momentum fraction carried by the quarks and antiquarks in the nucleon. There are recent measurements of the ratio of cross sections for the reactions $\nu_\mu N \rightarrow \mu^- X$ and $\bar{\nu}_\mu N \rightarrow \mu^+ X$ by the Caltech Fermilab³⁰ and CERN-Dortmund-Heidelberg-Saclay (CDHS)³¹ neutrino experiments, which obtained the values $\sigma_{\nu N}/\sigma_{\bar{\nu} N} = 0.476 \pm 0.019$ and 0.48 ± 0.03 , respectively (in the latter case the value corresponds to the energy range $30 < E < 90 \text{ GeV}$). From these measurements one obtains $\alpha \equiv \bar{Q}/Q \approx 0.17$ (with a small increase in this effective parameter α , as a function of E , being understood).³² It then follows that $\langle y \rangle \approx 0.49$ and 0.33 for $\eta = 1$ and -1 , respectively. In the spirit of our approximate analytical discussion these results may be applied to muon reactions. Using $E_{M^0} = (1-y)E$ and $E_H = yE$, we find that for $E = 225 \text{ GeV}$, $\langle E_{M^0} \rangle \approx 115$ and 150 GeV for $\eta = 1$ and -1 , respectively, while $\langle E_H \rangle \approx 110$ and 75 GeV , for the same values of η . Recall that $\eta = +1$ for cases (A), (B), and (C), while $\eta = -1$ for case (A'). When the $(\bar{M})^0$ decays to $\mu^- \mu^+ (\bar{\nu})_\mu$, if each of the three resulting leptons were emitted isotropically in the $(\bar{M})^0$ rest frame, they would, on the average, have a laboratory energy equal to $E_{M^0}/3$. Although the decay is not isotropic, this value of the final lepton energy provides a useful crude estimate of the actual average value: $\langle E_{\mu^\pm} \rangle \sim \langle E_{\nu, \bar{\nu}} \rangle \approx \langle E_{\text{missing}} \rangle \sim \langle E_{M^0, \bar{M}^0}/3 \rangle$. For $E = 225 \text{ GeV}$ these average energies have the values $\sim 40 \text{ GeV}$ and $\sim 50 \text{ GeV}$ for $\eta = 1$ and -1 , while for $E = 129 \text{ GeV}$, they have the correspondingly reduced values $\sim 20 \text{ GeV}$ and $\sim 30 \text{ GeV}$. These results will be useful in appraising the actual Monte Carlo calculations, in particular, the effect of the heavy-lepton and possible heavy-quark masses.

In Fig. 1 we present our calculation of the distributions in E_{μ^-} , E_{μ^+} , the hadronic energy E_H , and the visible energy E_{vis} , for the three reactions under consideration. Specifically, Figs. 1(a), 1(c), and 1(e) refer to reactions (A), (B), and (C) with $m_{M^0} = 4 \text{ GeV}$, while Figs. 1(b), 1(d), and 1(f) represent the same reactions, but with $m_{M^0} = 8 \text{ GeV}$. We have incorporated the cuts $E_\mu > 20 \text{ GeV}$ and $E_H > 20 \text{ GeV}$, which are characteristic of the BFP experiment; these appear as the vertical lines at which the muon and hadron energy curves end.²⁸ The units on the vertical

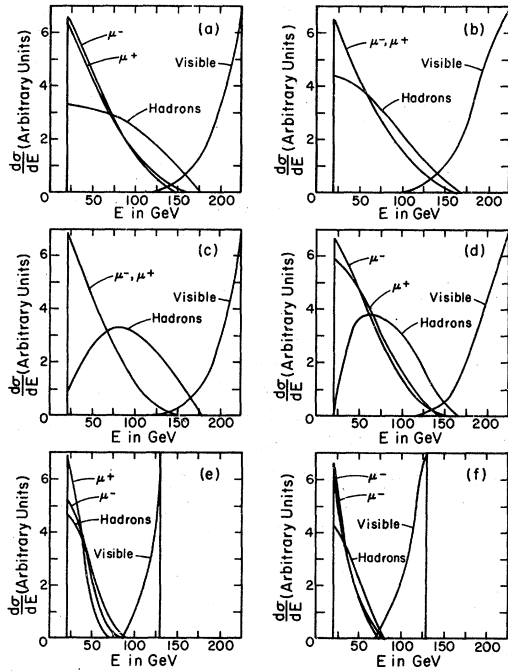


FIG. 1. Distributions in E_{μ^\pm} , E_H , and E_{vis} for dimuons from (\bar{M}^0) production and decay. Graphs (a), (c), and (e) represent reactions (A), (B), and (C), respectively, for $m_{M^0} = 4$ GeV; graphs (b), (d), and (f) represent the same reactions, but with $m_{M^0} = 8$ GeV. The lower bounds on the energies are set by the cuts $E_{\mu^\pm} > 20$ GeV and $E_H > 20$ GeV.

scales are arbitrary, since it is the shapes of the various distributions which are of primary interest. However, one should note that the event rates for reactions (B) and (C) are considerably smaller than that for reaction (A). It is evident from Fig. 1 that even for reaction (A), in which the heavy lepton and (in this case, light) quark mass effects are smallest, E_{μ^\pm} and E_H are somewhat smaller than the values obtained from the approximate analytical treatment. The reason for this is that even in this reaction the lepton mass still has a significant effect. Observe that the hadron energy in cases (A) and (C) is a monotonically decreasing function, whereas, in contrast, it exhibits a marked peak in case (B). This reflects the fact that the former two cases are (L, q) reactions, while case (B) is an (L, Q) process in which the heavy-quark mass is m_b . There are small differences between the μ^- and μ^+ spectra in Figs. 1(a)–1(f); these will be analyzed further below. As expected, the E_{μ^\pm} curves for the case $m_{M^0} = 8$ GeV extend to slightly greater energy than do those for the case $m_{M^0} = 4$ GeV.

There are two especially important conclusions to be drawn from these graphs. First, the μ^\pm energy is quite high, particularly for the cases in which $E = 225$ GeV. This fact is useful in distin-

guishing a dimuon signal arising from the (\bar{M}^0) apart from dimuons coming from various background sources, since in general the latter will not yield such high-energy dimuons. This applies, for example, to the μ^\pm from decays of π 's and K 's produced in the hadronic shower. Secondly, there is substantial missing energy carried off by the neutrino in the decay of the (\bar{M}^0) ; typically, for $E = 225$ GeV, $E_{missing} \sim 50$ GeV. As expected, $E_{missing}$ increases as a function of m_{M^0} . In reaction (A'), not shown in the figures, E_{μ^\pm} and $E_{missing}$ are greater than in reaction (A) by the ratio of M^0 energies, roughly 1.4. The large amount of missing energy serves as the basis for the crucial cut $E_{missing} > 20$ GeV. The reason for choosing this cutoff value of $E_{missing}$ is that the present BFP calorimeter is only capable of distinguishing a missing energy in excess of ~ 15 GeV from zero.²⁸

In addition to the individual muon energies and total missing energy, an important quantity which can be used to isolate the dimuon signal from possible (\bar{M}^0) production and decay is the correlation between the muon energies. It was, indeed, this correlation which played a significant role in confirming that the great majority of dilepton events observed in neutrino reactions are due to charm production and semileptonic decay, rather than to (\bar{M}^0) production. As was shown by Pais and Treiman,¹⁶ if a dimuon pair results from (\bar{M}^0) decay, then the ratio of the average muon energies satisfies the bound $0.48 < \langle E_{\mu^-} \rangle / \langle E_{\mu^+} \rangle < 2.10$. This bound expresses the fact that if the dimuon pair arises from a common parent, then the energies will be comparable. In contrast, in either a neutrino- or muon-induced reaction, if one muon arises from the leptonic vertex while the other arises from the semileptonic decay of a charmed hadron, then, as has been shown by theoretical simulations, the directly scattered muon will have substantially higher energy.³³ And, indeed, in $\sim 90\%$ of the dilepton events in (anti)neutrino reactions, this large energy asymmetry is observed.¹⁹

In Fig. 2 we present our results on the dimuon energy or momentum correlations in terms of two-dimensional scatter plots and energy asymmetry graphs. Figures 2(a), 2(c), and 2(e) are plots of the muon momenta p_{ss} versus p_{os} , where the subscripts "ss" and "os" denote "same sign" and "opposite sign" relative to the sign of the incident muon, for reactions (A), (B), and (C), respectively. The mass of the (\bar{M}^0) is taken to be 4 GeV for this figure. As is evident in the graphs, the cut $p_{\mu^\pm} > 20$ GeV has been incorporated. The salient feature of Figs. 2(a) and 2(c) is that it is equally probable for p_{ss} to be larger

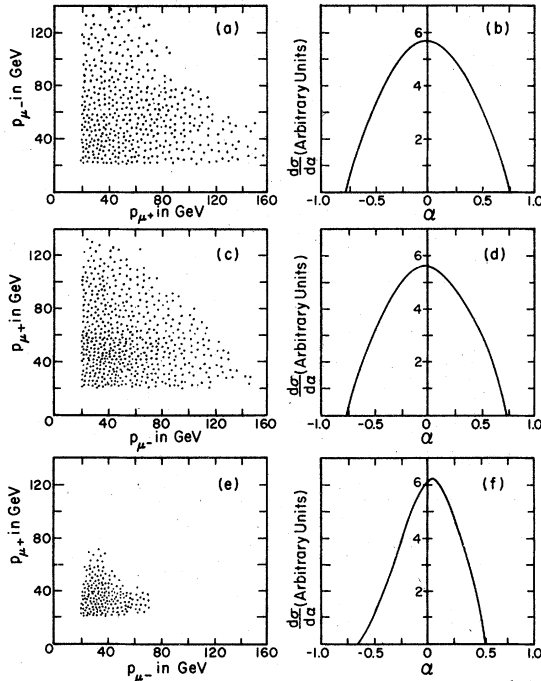


FIG. 2. Plots of dimuon energy correlations. Graphs (a), (c), and (e) are scatter plots of p_{ss} versus p_{os} for reactions (A), (B), and (C), respectively. Graphs (b), (d), and (f) are distributions in the muon momentum (or energy) asymmetry $\alpha \equiv [p(\mu_{ss}) - p(\mu_{os})] / [p(\mu_{ss}) + p(\mu_{os})]$ for the same reactions. The M^0 mass is taken to be 4 GeV for these graphs.

or smaller than p_{os} . In fact, there is a small asymmetry in the muon momenta in Fig. 2(e) (which will be explained below), but it is difficult to discern in this graph. The muon momentum or energy asymmetry is characterized more concisely in Figs. 2(b), 2(d), and 2(f), which are plots of the asymmetry parameter

$$\alpha \equiv \left(\frac{p_{ss} - p_{os}}{p_{ss} + p_{os}} \right) \quad (4.2)$$

for reactions (A), (B), and (C), respectively. By general arguments the average value $\langle \alpha \rangle = 0$ for cases (A) and (B), or more generally, for any decay in which $\chi_1 \chi_2 = -1$, i.e., the vertices involved in the decay are of opposite chirality. (Note that the Monte Carlo distributions do not reproduce this feature exactly; this is a result of the finite statistics in the calculation.) For reaction (C), on the other hand, an elementary helicity argument shows that $p_{\mu^-} > p_{\mu^+}$. The inequality $p_{ss} > p_{os}$ holds for any leptonic decay of (\bar{M}^0) in which $\chi_1 \chi_2 = 1$, which can be conveniently illustrated using reaction (C). At high energies the M_L^0 tends to be produced with helicity $\eta = -1$. Hence, in its decay the μ^+ is emitted preferentially into the backward hemisphere; indeed, the kinematical

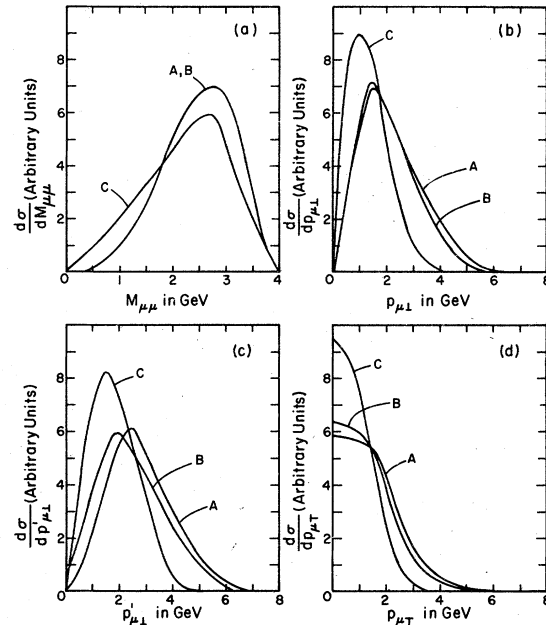


FIG. 3. Distributions in (a) dimuon invariant mass $M_{\mu\mu}$ and transverse momenta of the opposite-sign muon (b) $p_{\mu L}$, (c) $p'_{\mu L}$, and (d) $p_{\mu T}$. The three curves in each graph apply for reactions (A), (B), and (C), as labeled. For these plots $m_{M^0} = 4$ GeV.

configuration in which the μ^+ goes directly forward is forbidden by angular momentum conservation. Thus the α distribution for reaction (C) peaks at a nonzero, slightly positive value of α . However, the magnitude of the momentum asymmetry is evidently rather small. The importance of these dimuon energy of momentum correlations shown in Fig. 2 is that they indicate that dimuons arising from the decay of an (\bar{M}^0) have energies which are comparable, either as represented on a two-dimensional plot or in terms of an asymmetry variable. This in turn provides a valuable means of distinguishing these dimuons from those due to certain backgrounds, especially those in which one muon is directly produced at the leptonic vertex and the other arises from the hadronic shower.

Another important set of kinematic distributions involves the invariant mass and transverse momenta of the dimuon pair. In Figs. 3 and 4 we present our Monte Carlo calculations of these distributions, again for the three reactions (A), (B), and (C), and for $m_{M^0} = 4$ GeV in Fig. 3 and 8 GeV in Fig. 4. As is clear from Figs. 3(a) and 4(a), the distribution in invariant mass $M_{\mu\mu}$ has an energy-independent upper bound, which is in fact just the mass of the parent (\bar{M}^0) . This characteristic serves as a key indicator of (\bar{M}^0) production and stands in sharp contrast to the invariant-mass distributions for dimuons from the

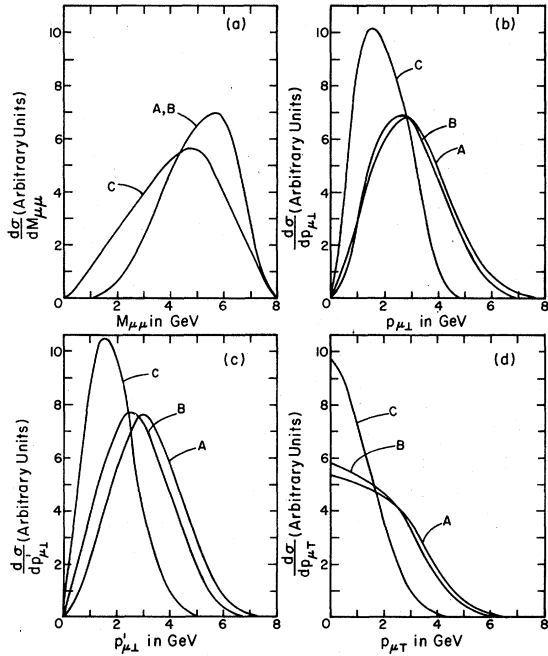


FIG. 4. Same distributions as in Fig. 3, but with $m_M^0 = 8$ GeV.

backgrounds which satisfy the missing energy cut, since these will always have energy-dependent upper bounds. It might be mentioned parenthetically that the invariant-mass distribution, like the ratio of muon energies, was one of the experimental determinants which were used to prove that the dominant part of the observed dilepton events in neutrino reactions was satisfactorily accounted for by the hypothesis of charm production, but not by the alternate hypothesis of $(\bar{M})^0$ production and leptonic decay.

The transverse momenta of the dimuons from the $(\bar{M})^0$ provide an important diagnostic quantity for the recognition of the heavy-lepton signal. One can analyze the transverse momenta of either the same-sign or the opposite-sign muons; we shall choose the latter here. There are then three useful types of transverse momenta. The first of these is the momentum of the opposite-sign muon transverse to the direction \hat{n}_b of the incident muon beam:

$$\vec{p}_{\mu\perp} \equiv \vec{p}_{os} - (\vec{p}_{os} \cdot \hat{n}_b) \hat{n}_b. \quad (4.3)$$

Analogously, one may define the momentum of the opposite-sign muon transverse to the apparent momentum-transfer direction $\hat{q}_{vis} \equiv (E\hat{n}_b - \vec{p}_{ss}) / |E\hat{n}_b - \vec{p}_{ss}|$:

$$\vec{p}'_{\mu\perp} \equiv \vec{p}_{os} - (\vec{p}_{os} \cdot \hat{q}_{vis}) \hat{q}_{vis}. \quad (4.4)$$

Finally, it is informative to consider the momentum of the opposite-sign muon transverse to

the apparent "production plane" (pp) defined by the directions of the incident beam and scattered same-sign muon:

$$\vec{p}_{\mu T} \equiv (\vec{p}_{os} \cdot \hat{n}_{pp}) \hat{n}_{pp}, \quad (4.5)$$

where

$$\hat{n}_{pp} \equiv \frac{(\hat{n}_b \times \vec{p}_{ss})}{|\hat{n}_b \times \vec{p}_{ss}|}. \quad (4.6)$$

From Figs. 3(b) and 4(b) one can see that the values of $p_{\mu\perp}$ are substantial: $\langle p_{\mu\perp} \rangle \approx 2$ (3) GeV for a 4 (8) GeV $(\bar{M})^0$ produced by an incident 225-GeV μ^\pm in reactions (A) and (B). As is reasonable, $\langle p_{\mu\perp} \rangle$ is smaller for reaction (C) because of the smaller incident muon energy, 129 GeV. Since the produced $(\bar{M})^0$ and the hadron spray recoil away from each other on opposite sides of the beam direction, and since the muons from the decay of the heavy lepton tend to follow its direction of motion, one would expect that $\langle p'_{\mu\perp} \rangle$ should be somewhat larger than $\langle p_{\mu\perp} \rangle$. Figures 3(c) and 4(c) verify this expectation. As is the case with $p_{\mu\perp}$, there is a gradual increase in $p'_{\mu\perp}$ as a function of the $(\bar{M})^0$ mass. Finally, Figs. 3(d) and 4(d) illustrate the $p_{\mu T}$ distribution. In contrast to the other two types of transverse-momentum distributions, $d\sigma/dp_{\mu T}$ is peaked at $p_{\mu T} = 0$. This can be understood as a consequence of the fact that $p_{\mu T}$ is the momentum transverse to a plane, whereas $p_{\mu\perp}$ and $p'_{\mu\perp}$ are momenta transverse to single direction vectors. Hence, there is much more phase space available for the kinematic configuration in which $p_{\mu T} = 0$ than there is for the configurations in which $p_{\mu\perp} = 0$ or $p'_{\mu\perp} = 0$.

The large values of transverse momenta of the muons arising from $(\bar{M})^0$ decay serve as another helpful means of isolating the heavy-lepton signal from certain backgrounds. For example, one type of background consists of dimuons in which one (the same-sign) member is the direct, electromagnetically scattered muon, and the other (opposite-sign) member arises from the decays of π 's and K 's produced in the hadronic shower. Another type consists of the direct, electromagnetically scattered muon together with an opposite-sign muon which is due to associated charm production in which one of the charmed hadrons decays (semi) leptonically. In both cases the values of $p_{\mu\perp}$, $p_{\mu T}$, and especially $p'_{\mu\perp}$, are significantly smaller than those for dimuons from $(\bar{M})^0$ decay. Note that for both of these backgrounds $\hat{q}_{vis} = \hat{q}$.

We proceed next to consider the azimuthal angle distributions. As before, there are two natural azimuthal angles; first, the one between the components of the two muon momenta normal to the beam direction \hat{n}_b :

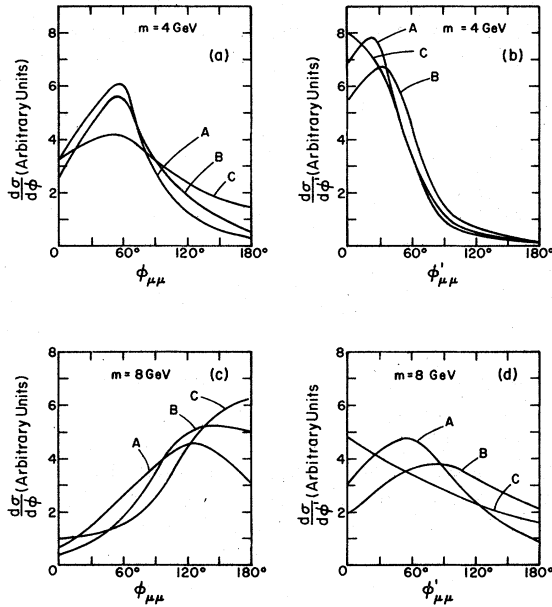


FIG. 5. Distributions in the azimuthal angles $\phi_{\mu\mu}$ and $\phi'_{\mu\mu}$ between the components of the muon momenta perpendicular to the beam and \hat{q}_{vis} directions, respectively. The three curves in each graph apply for the reactions (A), (B), and (C), as labeled. The M^0 mass is taken to be 4 GeV for graphs (a) and (b), and 8 GeV for graphs (c) and (d).

$$\phi_{\mu\mu} \equiv \sin^{-1} \left[\frac{|(\vec{p}_{ss})_{\perp} \times (\vec{p}_{os})_{\perp}|}{|(\vec{p}_{ss})_{\perp}| \cdot |(\vec{p}_{os})_{\perp}|} \right] \quad (4.7)$$

and, secondly, the analogous azimuthal angle between the components of the muon momenta normal to the \hat{q}_{vis} direction:

$$\phi'_{\mu\mu} \equiv \sin^{-1} \left[\frac{|(\vec{p}_{ss})_{\perp qv} \times (\vec{p}_{os})_{\perp qv}|}{|(\vec{p}_{ss})_{\perp qv}| \cdot |(\vec{p}_{os})_{\perp qv}|} \right]. \quad (4.8)$$

In Fig. 5 we present our Monte Carlo results for the $\phi_{\mu\mu}$ and $\phi'_{\mu\mu}$ distributions, for each of the three reactions (A), (B), and (C), and for $m_{M^0} = 4$ GeV and 8 GeV, respectively. The qualitative features of these graphs are easily understood. For small values of $m_{M^0}^2/(2m_N E)$, i.e., muon energies far above threshold for a given heavy-lepton mass m_{M^0} , the (\bar{M}^0) is produced with substantial transverse momentum relative to the beam direction. As may be recalled from reference to Figs. 3 and 4, since the (\bar{M}^0) and W boson or hadron spray recoil on opposite sides of the beam direction, the transverse momentum of the (\bar{M}^0) relative to the hadron spray is even larger than that relative to the beam direction. Since the muons from the decay of the heavy lepton tend to follow its path, the azimuthal angle $\phi_{\mu\mu}$ between them is rather small, and $\phi'_{\mu\mu}$ is commensurately somewhat smaller. For example, the $\phi_{\mu\mu}$ and $\phi'_{\mu\mu}$ distributions in Figs. 5(a) and

5(b) peak at roughly 60° and 0° – 30° , respectively. However, for larger values of the quantity $m_{M^0}^2/(2m_N E)$, i.e., energies not too far above threshold for a given m_{M^0} , the heavy lepton is constrained to travel essentially forward along the beam direction. The two muons are thus emitted with a large azimuthal angle between them, and accordingly, $\phi_{\mu\mu}$ peaks at $\sim 150^\circ$ – 180° . Nevertheless, as one can see from Fig. 5(d), even in this case, because of the larger transverse momentum relative to the hadronic spray direction, the angle $\phi'_{\mu\mu}$ tends to have values considerably smaller than those at which the maxima of the $\phi_{\mu\mu}$ curves occur.

The kinematic information contained in these azimuthal-angle distributions is similar to that in the transverse-momentum distributions. The general feature to note is that for energies a reasonable distance above threshold, the angles $\phi_{\mu\mu}$ and $\phi'_{\mu\mu}$ tend to be rather small. It is important here to remember that although for clarity the vertical scales on the graphs of all the one-variable distributions, and in particular, the graphs of $d\sigma/d\phi_{\mu\mu}$ and $d\sigma/d\phi'_{\mu\mu}$, are marked in conveniently chosen arbitrary units, in fact the absolute rate for the case $m_{M^0} = 4$ GeV is much larger than for the case $m_{M^0} = 8$ GeV. More generally, for a given heavy-lepton mass, if one considers the energy as a variable, by far the dominant contribution to the cross section will come from high energies, and hence the resulting dimuons will be characterized by small values of $\phi_{\mu\mu}$ and $\phi'_{\mu\mu}$. In contrast, background dimuons formed by an electromagnetically scattered muon together with an opposite-sign muon from π , K , or charm decay in the hadronic shower, will be characterized by large values of $\phi_{\mu\mu}$ and $\phi'_{\mu\mu}$. Thus these azimuthal-angle plots serve as yet another powerful tool for separating the possible (\bar{M}^0) signal from various backgrounds.

Finally, Figs. 6, 7, and 8 are scatter plots of $p_{\mu T}$ versus $M_{\mu\mu}$, $\phi_{\mu\mu}$, and $\phi'_{\mu\mu}$, respectively. In each figure, graphs (a), (c), and (e) represent reactions (A), (B), and (C), with $m_{M^0} = 4$ GeV, while graphs (b), (d), and (f) represent the same reactions, but with $m_{M^0} = 8$ GeV. Figure 6 shows the feasibility of imposing a cut $p_{\mu T} > 1$ GeV, which is very helpful in suppressing background sources of dimuons. From Figs. 7 and 8 one can see that the smallest values of $\phi_{\mu\mu}$ and $\phi'_{\mu\mu}$ for high incident muon energies, and the largest values of these angles in the contrasting low-energy case, occur at low values of $p_{\mu T}$. Thus the possible cuts which one could make, viz. $p_{\mu T} > 1$ GeV and, for the relevant high-energy case, $\phi_{\mu\mu} < 90^\circ$ and $\phi'_{\mu\mu} < 90^\circ$, are somewhat complementary.

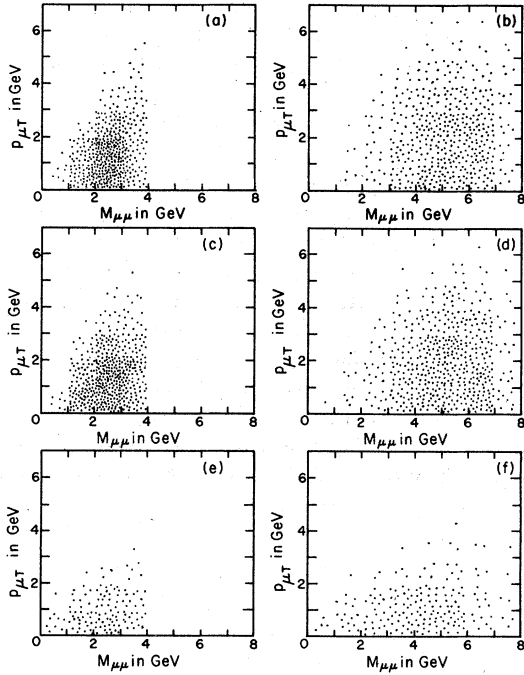


FIG. 6. Scatter plots in the transverse momentum of the opposite-sign muon, $p_{\mu T}$, versus the dimuon invariant mass $M_{\mu\mu}$. Graphs (a), (c), and (e) represent reactions (A), (B), and (C), respectively, with $m_{M^0}=4$ GeV; graphs (b), (d), and (f) represent the same reactions, but with $m_{M^0}=8$ GeV.

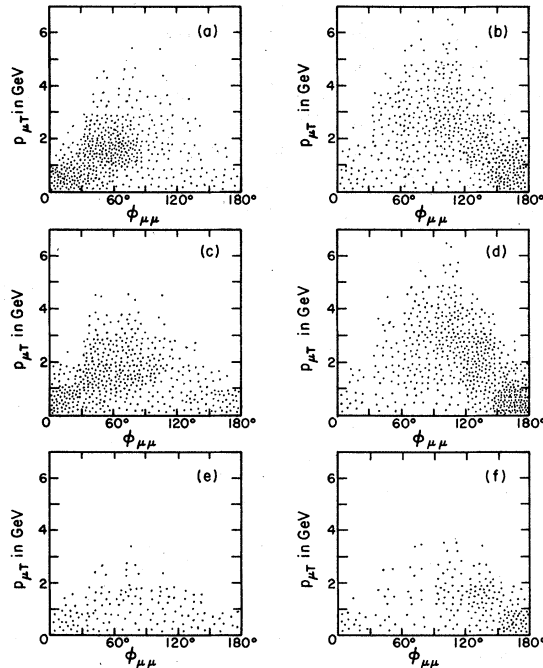


FIG. 7. Scatter plots in the transverse momentum $p_{\mu T}$ of the opposite-sign muon versus the azimuthal angle $\phi_{\mu\mu}$. The reaction and M^0 mass represented in each graph are as in Fig. 6.

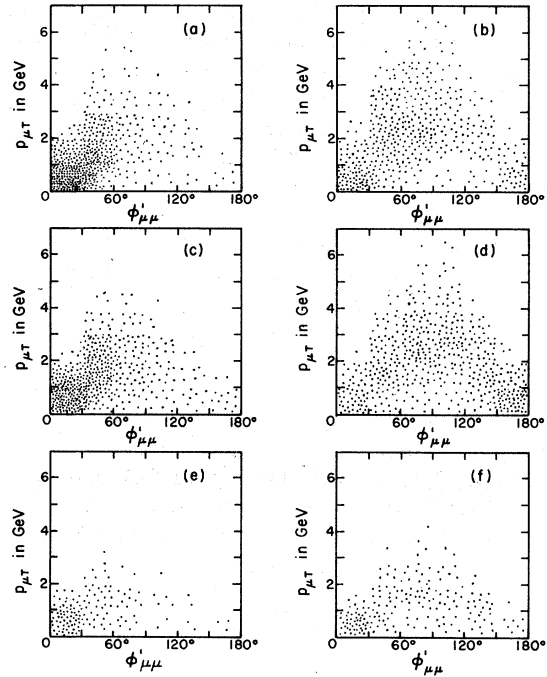


FIG. 8. Scatter plots in the transverse momentum $p_{\mu T}$ of the opposite-sign muon versus the azimuthal angle $\phi'_{\mu\mu}$. The reaction and M^0 mass represented in each graph are as in Fig. 6.

Thus, our distributions in E_{μ^\pm} , E_H , E_{vis} , $M_{\mu\mu}$, $p_{\mu\perp}$, $p'_{\mu\perp}$, $p_{\mu T}$, $\phi_{\mu\mu}$, and $\phi'_{\mu\mu}$ give a reasonably complete description of the characteristics of the dimuon signal from the muon-induced production and leptonic decay of a neutral heavy lepton (\bar{M}^0) . They exhibit several distinctive features which may be recalled here: (1) large values of E_{μ^\pm} and $E_{missing}$; (2) comparable values of $E(\mu_{ss})$ and $E(\mu_{os})$; (3) an energy-independent upper bound to the invariant-mass distribution, which is the mass of the parent (\bar{M}^0) ; (4) substantial values of $p_{\mu\perp}$, $p_{\mu T}$, and especially $p'_{\mu\perp}$ (assuming the lepton mass to be 4 or 8 GeV and the incident muon energy to be 225 GeV); and (5) small values of the azimuthal angles $\phi_{\mu\mu}$ and $\phi'_{\mu\mu}$ (assuming that the incident muon energy is sufficiently far above threshold that the event rate is non-negligible). These characteristics are important because they indicate the ways in which one can distinguish the possible heavy-lepton-induced dimuon events from those due to various backgrounds. We shall next describe the features of the main backgrounds.

V. BACKGROUNDS AND CONCLUDING REMARKS

As was stressed at the beginning of this paper, the expected rate for the process $\mu^\pm N \rightarrow (\bar{M}^0) X$, $(\bar{M}^0) \rightarrow \mu^\mp \mu^\pm X$, with $m_{M^0} \sim 4-8$ GeV and $E = 225$ GeV, is of order $\sim 10^{-6}$ of the regular electromagnetic

process $\mu^\pm N \rightarrow \mu^\pm X$. Consequently, in order to be able to obtain a reasonable number of $(\bar{M})^0$ -generated dimuons, it is necessary to have a muon beam with the highest possible intensity. As regards the background problem, the tiny relative rate is not, by itself, a fatal shortcoming, since the electromagnetic muon reaction will never yield a $\mu^- \mu^+$ pair. The problem, of course, is that there are a number of higher-order processes which build upon the basic electromagnetic reaction and can yield such a dimuon pair. However, if one triggers on a $\mu^- \mu^+$ pair, imposes the usual cuts on E_{μ^\pm} , E_H (and the geometrical cut on θ_{μ^\pm}), and requires that (1) there be substantial missing energy, $E_{\text{missing}} > 20$ GeV; (2) the average muon energies satisfy the Pais-Treiman bound¹⁶ $0.48 < \langle E_{\mu^-} \rangle / \langle E_{\mu^+} \rangle < 2.1$; (3) $p_{\mu^\pm}^{\perp} \gtrsim 1$ GeV and/or $p_{\mu T} \gtrsim 1$ GeV; and (4) $Q_{\text{vis}}^2 > 10$ –15 GeV², then one has a good chance of eliminating background dimuons and isolating a dimuon signal from the production and leptonic decay of an $(\bar{M})^0$. We recall the functions of these cuts: the E_{μ^\pm} cut rejects muons from the decays of π 's and K 's produced in the hadronic shower and guarantees that the fractional error in the measurement of the muon momenta is tolerably small. The E_H cut ensures that the process is deeply inelastic, while the crucial E_{missing} cut is designed to select events with a missing neutrino. The cuts on $\langle E_{\mu^-} \rangle / \langle E_{\mu^+} \rangle$ and on the transverse momenta of the opposite-sign muon are intended to isolate dimuons from $(\bar{M})^0$ decay. Finally, the cut on Q_{vis}^2 is very effective in eliminating backgrounds, since the only important backgrounds involve the basic electromagnetic scattering process $\mu^\pm N \rightarrow \mu^\pm X$, for which the rate falls off sharply as a function of $Q_{\text{vis}}^2 = Q^2$. The geometrical cut on θ_{μ^\pm} expresses the requirement that the muons must not scatter at so large an angle that their momenta are not measured or they are not definitely identified as muons.

The important backgrounds can be classified under two categories: (a) $\mu^\pm N \rightarrow \mu^\pm X(Y)$, $Y \rightarrow \mu^\mp X$, and (b) $\mu^\pm N \rightarrow \mu^\pm X(Y)$, $Y \rightarrow \mu^- \mu^+ X$, where one of the same-sign muons is missed, leaving an apparent $\mu^- \mu^+$ pair. Here X denotes, as usual, an arbitrary final hadronic state, and Y denotes an unspecified source of a muon or dimuon pair, which may or may not be part of the state X . In practice Y is a π , K , charmed hadron, τ lepton, or virtual photon, γ_ν . Let us now consider the specific backgrounds in turn.

The first background consists of dimuons of type (a) in which the same-sign member is a direct, electromagnetically scattered muon, and the opposite-sign member arises from the decay of a π or K produced in the hadronic spray. It is

very unlikely for a single pion or kaon to carry a substantial fraction of the hadronic energy E_H which would be necessary to yield a high-energy muon and a neutrino that could carry away a considerable amount of energy. Indeed, if the meson were sufficiently energetic for these conditions to be met, then its decay length would far exceed its interaction length and, in fact, the length of the detector. Hence, only very low-energy pions and kaons will decay before interacting or escaping. In turn, the resulting muon will fail the cut on E_{μ^\pm} , and the neutrino will not carry off enough energy to satisfy the cut on E_{missing} . As regards the relative energies of the leading and slow muons, $E(\mu_{\text{ss}})/E(\mu_{\text{os}})$ will be quite large, typically of order 10^2 for an incident muon energy of 225 GeV. Hence the Pais-Treiman test¹⁶ will be strongly violated, showing clearly that the event did not arise from an $(\bar{M})^0$. The cuts on Q_{vis}^2 and E_H will also very severely suppress this background. Other useful features include the fact that the slow, opposite-sign muon is produced with quite small transverse momentum relative to the hadron spray direction; $p_{\mu^\pm}^{\perp} \lesssim 0.3$ GeV. This contrasts sharply with the values of $p_{\mu^\pm}^{\perp}$ for opposite-sign muons from an $(\bar{M})^0$. Similar comments apply to the azimuthal angle correlation; $\phi_{\mu\mu}$ will be large, of order 180° , for this background, again in clear contrast to the generally small values of $\phi_{\mu\mu}$ for the $(\bar{M})^0$ signal. Finally, two standard methods of eliminating dimuons from pion and kaon decays are the test for uniformity of events as a function of longitudinal position in the detector, and the variable density test.¹⁹ These have been used extensively in past experiments on (anti)neutrino-induced dimuon production. Thus, this first background does not seem to be serious.³⁴

A second background consists of the electromagnetic reaction $\mu^\pm N \rightarrow \mu^\pm X$, in which associated charm production occurs, and one of the charmed hadrons, "C", decays via the (semi)leptonic mode $(\bar{C}) \rightarrow \mu^\pm (\bar{\nu})_\mu \dots$ to yield an opposite-sign dimuon pair, together with some missing energy. Alternatively, both the C and \bar{C} hadrons might decay to yield muons, but in such a way that one of the two resulting same-sign muons is missed. Since associated charm production in neutrino reactions is a potential source of trimuons, there has been considerable interest recently in determining its rate. For the high-energy portion of a neutrino spectrum ($E_\nu > 100$ GeV), after cuts of $E_{\mu^\pm} > 4$ GeV have been folded in, it has been found that the cross section for trimuon production via associated charm production and (semi)leptonic decay is $\lesssim 10^{-5}$ of the corresponding charged current cross section.³⁵

In order to obtain the contribution to opposite-sign dimuon production, we divide by a typical charmed hadron semileptonic branching ratio, $B(D \rightarrow e^+ X) \approx 0.1$ and get a rough estimate of $\sim 10^{-4}$. To apply this number to the electromagnetic background process of interest here, it is important to take account of the fact that the BFP experiment imposes a much higher cut on muon energy, $E_{\mu^\pm} > 20$ GeV, than the ~ 4 -GeV cuts applied in the neutrino experiments and the corresponding calculations of Ref. 35. We expect that this will reduce the contribution of associated charm production to apparent opposite-sign dimuon pairs in the BFP experiment to a level $< 10^{-5}$ of the rate for the basic reaction $\mu^\pm N \rightarrow \mu^\pm X$. Concerning spectral characteristics, in contrast to the first background, E_{missing} and p_{\perp} are not negligible here, but they are still smaller than would be the case for dimuons from an $(\bar{M})^0$. Moreover, it is well established from data on neutrino-induced dimuons that the muon from charm decay has a considerably smaller energy than the muon which is produced directly at the leptonic vertex.³³ In electromagnetic reactions y is substantially smaller than in neutrino reactions because of the preference for low $Q^2 = 2m_N E x y$. Consequently, the ratio $E(\mu_{\text{ss}})/E(\mu_{\text{os}})$ will be even larger for the background under discussion than for dimuons from charm production in neutrino reactions. Thus, the Pais-Treiman test¹⁶ can be used quite effectively to eliminate this second background. The cut on Q_{vis}^2 and a possible cut $\phi_{\mu\mu} < 90^\circ$ also strongly suppress these background dimuons. Finally, since associated charm production yields equal numbers of μ^- and μ^+ , this process will produce essentially equal numbers of same-sign and opposite-sign dimuons. Hence, another very effective way of rejecting this background is to subtract the observed same-sign dimuons from the opposite-sign ones. (Note that pion and kaon decay do not yield exactly equal numbers of μ^- and μ^+ because of the larger interaction cross sections for π^- and K^- than for π^+ and K^+ .)

A third background, of type (b) according to the classification given above, arises from the production of opposite-sign dimuon pairs by virtual photons, which in turn are produced via emission from leptons or hadrons (quarks), via quark-antiquark annihilation, or via the Bethe-Heitler process. If one of the two resulting same-sign muons is missed, these mechanisms will yield apparent opposite-sign dimuon events. As was the case with associated charm production, this background (excluding the contributions due to virtual-photon emission from the initial lepton line and the Bethe-Heitler process) yields trimuons in neutrino reactions and has consequently

been studied with care recently.^{36,37} One can crudely estimate that, neglecting the effects of cuts, the rate for trimuon production via this process is of order $\alpha^2 \approx 5 \times 10^{-5}$ smaller than the rate for the reaction $(\bar{\nu})_{\mu} N \rightarrow \mu^\pm X$. Detailed Monte Carlo calculations agree approximately with this rough estimate; for the cuts and neutrino spectrum of the CDHS experiment they give³⁶ $\sigma(\nu_{\mu} N \rightarrow \mu^- \mu^- \mu^+ X) / \sigma(\nu_{\mu} N \rightarrow \mu^- X) \approx 3 \times 10^{-5}$. In order to use this result for our present background estimate, we need to know what fraction of the trimuons will appear as opposite-sign dimuons. In the BFP experiment the two main ways in which this can happen are the following: (1) if one muon is produced travelling in essentially the same direction and with essentially the same energy as another muon of the same sign, so that the two tracks cannot definitely be resolved, and (2) if one of the same-sign muons has very low energy or large scattering angle, so that it cannot be identified as a muon. The related question of what fraction of neutrino-induced trimuon events due to various possible production mechanisms appear to be dimuons has been addressed previously.^{27,36} A similar analysis could be carried out here, incorporating the BFP muon energy and angle cuts. However, since the total muon detection efficiency depends in detail on the geometry and track-resolution capability of the BFP detector, it seems inappropriate to perform such a calculation in this paper. In lieu of this, we estimate that the fraction of electromagnetically generated trimuon events which would be classified as opposite-sign dimuons in the BFP experiment is of order²⁸ ~ 0.1 . Note that there is an additional uncertainty in this number due to the contributions of the Bethe-Heitler process and the radiation of a virtual photon from the initial lepton line, which are negligible or absent in the case of neutrino reactions, but are present in muon reactions. The resulting estimate for the contribution of electromagnetic muon pair production to opposite-sign dimuons satisfying the requisite cuts in the BFP experiment is $\sim 3 \times 10^{-6}$ of the event rate for the lowest-order electromagnetic muon scattering reaction. This number is understood to subsume the contributions of various exclusive channels, such as diffractive production of (self-conjugate) vector mesons which decay leptonically to dimuon pairs. Given the variety of electromagnetic mechanisms which can yield apparent dimuons, including virtual-photon emission from the leptons or hadrons, Bethe-Heitler production, and quark-antiquark annihilation, and given the two possible choices as to which same-sign muon is missed, it is clear that this general background can give

rise to dimuon events with a large range of values of $E(\mu_{ss})/E(\mu_{os})$, $p_{\mu L}$, $p'_{\mu L}$, $p_{\mu T}$, $\phi_{\mu\mu}$, and $\phi'_{\mu\mu}$.³⁸ Further, although the invariant mass of a dimuon pair from a virtual photon will tend to be very small, there are comparable probabilities that the observed dimuon will be comprised of this pair or, instead, a pair consisting of the directly scattered muon together with the opposite-sign muon from the virtual-photon-induced pair. Hence, some of the observed events will indeed be characterized by very small invariant mass $M_{\mu\mu}$, but a comparable number will not. Consequently, the main cut which can be used to suppress this source of background dimuons is the cut on Q_{vis} .² The cut on E_H is also effective in eliminating these events since, like the majority of electromagnetic events, they tend to have small energy transfer ν .

Finally, one may consider the analog of this third background in which the electromagnetically generated dimuon pair is replaced by a $\tau^- \tau^+$ pair. If the $\tau^- \tau^+$ pair decays to $\mu_{os} + (\text{anti})\text{neutrinos} + \text{possible hadrons}$, or if it decays leptonically to $\mu_{os} \mu'_{os} + (\text{anti})\text{neutrinos}$ and one of the same-sign muons is missed, then this process will produce an apparent opposite-sign dimuon event. Furthermore, such an event would often involve a sizable amount of missing energy and substantial values of the transverse momenta of the opposite-sign muon. However, it is easy to see that in fact this is a negligible background: For a $\tau^- \tau^+$ pair produced by a single virtual photon, the rate is of order $(m_\mu^2/m_\tau^2)^2 \approx 1 \times 10^{-5}$ smaller than the corresponding muon pair production rate. A similar argument applies for the case of $\tau^- \tau^+$ pairs generated via the Bethe-Heitler process.³⁹ Since, as has been argued above, the background due to electromagnetically generated muon pairs is expected to be tolerable, the background due to $\tau^- \tau^+$ pair production is negligible.

From this brief analysis of the main backgrounds we infer that the characteristics of dimuons from the high-energy muon-induced production and decay of an $(\bar{M})^0$ are sufficiently distinctive that, with the trigger and cuts discussed above, one

has a reasonable chance of isolating the heavy-lepton signal. Of course, this also requires a great-enough muon beam intensity and integrated running time to enable one to gather a significant sample of candidate dimuon events.

Thus, in conclusion, experiments with high-energy muon beams and accurate hadron calorimetry present an important opportunity to search for possible neutral heavy leptons of a kind not directly tested for by previous experiments. Such high-energy muon reactions are sensitive to $(\bar{M})^0$'s of much higher masses than neutrino experiments are (for the different kind of neutral heavy leptons which couple to neutrinos). We have analyzed the characteristics of the dimuon signal which could be used to carry out this search. The backgrounds, although important, do not appear to be prohibitively serious. Our analysis is applicable to the muon experiment currently being performed by a Berkeley-Fermilab-Princeton collaboration. Indeed, this experiment is the first one to be able effectively to apply one of the crucial tests for the heavy-lepton production and decay, namely the test for substantial missing energy. Although there is, at present, indirect evidence against the existence of neutral heavy leptons, there is no substitute for a direct experimental search for these particles. Hopefully the results of our study will be useful as part of this endeavor.

ACKNOWLEDGMENTS

We would like to thank S. Loken, F. Shoemaker, P. Surko, and M. Strovink for valuable discussions concerning the Berkeley-Fermilab-Princeton muon experiment. We are also grateful to J. Smith for helpful conversations. The research of C. H. A. was supported in part by the National Science Foundation under Grant No. PHY 77-07864 and in part by the Department of Energy. The research of R. E. S. was supported in part by the Department of Energy under Contract No. EY-76-C02-3072.

*Permanent address.

¹S. Weinberg, Phys. Rev. Lett. **19**, 1264 (1967); A. Salam, in *Elementary Particle Theory: Relativistic Groups and Analyticity* (Nobel Symposium No. 8), edited by N. Svartholm (Almqvist and Wiksell, Stockholm, 1968), p. 367.

²For recent reviews, see B. Barish, in *Proceedings of the International Symposium on Lepton and Photon Interactions at High Energies, Hamburg, 1977*, edited by F. Gutbrod (DESY, Hamburg, 1977); P. Musset,

ibid; C. Baltay, in *Proceedings of the XIX International Conference on High Energy Physics* (Phys. Soc. of Japan, Tokyo, 1978); S. Weinberg, *ibid*.

³A. M. Cnops *et al.*, Phys. Rev. Lett. **41**, 357 (1978). Although the original high-energy Gargamelle results, reported in J. Blietschau *et al.*, Phys. Lett. **73B**, 232 (1978), strongly disagreed with the WS model, assuming $\sin^2\theta_W \approx 0.24$ as required by the $\nu, \bar{\nu}$ NC/CC data, subsequent results from this experiment appear to be nearer to the WS predictions. The situation is re-

- viewed by C. Baltay (Ref. 2).
- ⁴C. Y. Prescott *et al.*, Phys. Lett. 77B, 367 (1978).
- ⁵See, e.g. N. Fortson, in *Neutrinos-78*, proceedings of the International Conference on Neutrino Physics and Astrophysics, Purdue University, edited by Earle C. Fowler (Purdue Univ., Lafayette, Indiana, 1978), p. 417.
- ⁶M. Kobayashi and T. Maskawa, Prog. Theor. Phys. 49, 652 (1973). The four-quark version of the WS model was first discussed by S. Glashow, J. Iliopoulos, and L. Maiani, Phys. Rev. D 2, 1285 (1970).
- ⁷M. L. Perl *et al.*, Phys. Rev. Lett. 35, 1489 (1975); G. Feldman *et al.*, *ibid.* 38, 117 (1977); M. L. Perl *et al.*, Phys. Lett. 63B, 466 (1976); 70B, 487 (1977). See also J. Burmeister *et al.*, *ibid.* 68B, 297 (1977); R. Brandelik *et al.*, *ibid.* 73B, 109 (1978); W. Bacino *et al.*, Phys. Rev. Lett. 41, 1 (1978).
- ⁸S. Herb *et al.*, Phys. Rev. 39, 252 (1977); Ch. Berger *et al.*, Phys. Lett. 76B, 243 (1978); C. Darden *et al.*, *ibid.* 76B, 246 (1978).
- ⁹V. Shvartsman, Zh. Eksp. Teor. Fiz. Pis'ma Red. 9, 315 (1969) [JETP Lett. 9, 184 (1969)]; G. Steigman, D. Schramm, and J. Gunn, Phys. Lett. 66B, 202 (1977); D. Schramm, Chicago report (unpublished).
- ¹⁰A. Clark, E. Groves, R. Johnson, L. Kerth, S. Loken, F. Shoemaker, P. Surko, M. Strovink, and W. Wenzel, Berkeley-Fermilab-Princeton Collaboration, Proposal for Fermilab Experiment 203-391 (unpublished).
- ¹¹Y. Watanabe *et al.*, Phys. Rev. Lett. 35, 898 (1975); C. Chang *et al.*, *ibid.* 35, 901 (1975).
- ¹²See, e.g., C. Chang *et al.*, Phys. Rev. Lett. 39, 519 (1977).
- ¹³H. Anderson *et al.*, Phys. Rev. Lett. 37, 4 (1976); 38, 1450 (1977).
- ¹⁴O. Allkofer *et al.* (E. Gabalthuler, spokesman), Proposal for CERN Experiment NA-2 (unpublished).
- ¹⁵F. Ceradini *et al.* (C. Rubbia, spokesman), Proposal for CERN Experiment NA-4 (unpublished).
- ¹⁶A. Pais and S. B. Treiman, Phys. Rev. Lett. 35, 1206 (1975); Phys. Rev. D 14, 293 (1976).
- ¹⁷For an example of a (now obsolete) model with an allowable type of nondiagonal neutral current, see B. W. Lee and S. Weinberg, Phys. Rev. Lett. 38, 1237 (1977); B. W. Lee and R. Shrock, Phys. Rev. D 17, 2410 (1978).
- ¹⁸D. Meyer *et al.*, Phys. Lett. 70B, 469 (1977).
- ¹⁹For recent reviews of dilepton production in neutrino reactions, see B. Barish, in *Proceedings of the International Symposium on Lepton and Photon Interactions at High Energies, Hamburg, 1977*, edited by F. Gutbrod (DESY, Hamburg, 1977); D. Cline, *ibid.*; C. Baltay, in *Proceedings of the XIX International Conference on High Energy Physics* (Phys. Soc. of Japan, Tokyo, 1978); K. Tittel, *ibid.*
- ²⁰C. H. Albright, Phys. Rev. Lett. 28, 1150 (1972); Phys. Rev. D 7, 63 (1973); 12, 1319 (1975); L.-N. Chang, E. Derman, and J. Ng, Phys. Rev. Lett. 35, 6 (1975); Phys. Rev. D 12, 3539 (1975); L. Sehgal and P. Zerwas, *ibid.* 16, 2379 (1977); D. Rein *et al.*, Nucl. Phys. B138, 85 (1978).
- ²¹D. Bechis *et al.*, Phys. Rev. Lett. 40, 602 (1978).
- ²²H. Georgi and H. D. Politzer, Phys. Rev. Lett. 36, 1281 (1976); Phys. Rev. D 14, A. De Rújula, H. Georgi, and H. D. Politzer, *ibid.* 15, 2495 (1977); D. Gross, S. B. Treiman, and F. Wilczek, *ibid.* 15, 2486 (1977).
- ²³Equation (3.3) is due to C. Callan and D. Gross, Phys. Rev. Lett. 22, 156 (1969).
- ²⁴S. Pakvasa, D. Parashar, and S. Tuan, Phys. Rev. D 10, 2124 (1974). The sea parton distribution has been modified to agree with the measurement by M. Holder *et al.*, Phys. Lett. 69B, 377 (1977). This change has a negligible effect on our calculations.
- ²⁵R. Field and R. P. Feynman, Phys. Rev. D 15, 2590 (1977).
- ²⁶C. H. Albright and J. Smith, Phys. Lett. 77B, 94 (1978).
- ²⁷C. H. Albright, R. Shrock, and J. Smith, Phys. Rev. D 17, 2383 (1978).
- ²⁸We thank S. Loken, F. Shoemaker, M. Strovink, and P. Surko for valuable discussions of the details of the Berkeley Fermilab-Princeton muon experiment.
- ²⁹For calculations of (anti) neutrino-induced charged heavy-lepton production and decay, see C. H. Albright and C. Jarlskog, Nucl. Phys. B84, 467 (1975); C. H. Albright, C. Jarlskog, and L. Wolfenstein, *ibid.* B84, 493 (1975). See also A. Soni, Phys. Rev. D 11, 624 (1975). For (anti) neutrino-induced neutral-heavy-lepton production, see Ref. 20. The case of (anti) neutrino-induced heavy-lepton and concomitant heavy-quark production is discussed in Ref. 27.
- ³⁰B. C. Barish *et al.*, Phys. Rev. Lett. 39, 1595 (1977).
- ³¹M. Holder *et al.*, Phys. Rev. Lett. 39, 433 (1977); K. Tittel, in *Proceedings of the XIX International Conference on High Energy Physics* (Phys. Soc. of Japan, Tokyo, 1978).
- ³²For recent reviews of charged-current neutrino data, see K. Tittel, Ref. 31; and A. K. Mann, in *Proceedings of the XIX International Conference on High Energy Physics* (Phys. Soc. of Japan, Tokyo, 1978).
- ³³The kinematic characteristics of dimuons from the (anti) neutrino-induced production, and decay of charmed hadrons are analyzed in E. Derman, Nucl. Phys. B110, 40 (1976); L. Sehgal and P. Zerwas, Phys. Rev. Lett. 36, 399 (1976); Nucl. Phys. B108, 483 (1976); L.-N. Chang, E. Derman, and J. Ng, Phys. Rev. D 16, 3157 (1977).
- ³⁴The background due to π and K decay has previously been estimated by Monte Carlo simulation in Ref. 10. For $E = 200$ GeV, $m_{M^0} = 4$ GeV, the branching ratio $B(M^0 \rightarrow \mu^+ \mu^- \nu_\mu) = 0.25$, and the cuts $E(\mu^+) > 20$ GeV, $E(\mu_{ss}) < 100$ GeV, $Q_{vis}^2 > 3.7$ GeV², and $p_{\mu 1} > 1.4$ GeV, it was found that the ratio of the dimuon rate from this background relative to that from the decay of the M^0 was $\sim 2\%$. As stated in the text, this relative rate can be further reduced by the cuts $E_{missing} > 20$ GeV, $0.48 < E_{\mu^-}/E_{\mu^+} < 2.1$, $p'_{\mu 1} > 1$ GeV, $\phi_{\mu\mu} > 90^\circ$, and depending on the experiment, a longitudinal uniformity or variable density test.
- ³⁵G. Kane, J. Smith, and J. Vermaseren, Phys. Rev. D 19, 1978 (1979) and references therein.
- ³⁶J. Smith and J. Vermaseren, Phys. Rev. D 17, 2288 (1978).
- ³⁷For reviews of the status of trimuon production in neutrino reactions, see K. Tittel, in *Proceedings of the XIX International Conference on High Energy Physics* (Phys. Soc. of Japan, Tokyo, 1978); A. K. Mann, *ibid.*; J. Smith, in *Neutrinos-78* (Ref. 5), p. 551.
- ³⁸For a recent discussion of electromagnetic trimuon production in muon reactions, see V. Ganapathi and J. Smith, Phys. Rev. D 19, 801 (1979).
- ³⁹The related case of $\tau^+\tau^-$ photoproduction is analyzed in J. Smith *et al.*, Phys. Rev. D 15, 648 (1977).